

Hybrid Protection of Digital FIR Filters

Levent Aksoy, *Member, IEEE*, Quang-Linh Nguyen, *Student Member, IEEE*, Felipe Almeida, Jaan Raik, *Member, IEEE*, Marie-Lise Flottes, *Member, IEEE*, Sophie Dupuis, *Member, IEEE*, and Samuel Pagliarini, *Member, IEEE*

Abstract—A digital Finite Impulse Response (FIR) filter is a ubiquitous block in digital signal processing applications and its behavior is determined by its coefficients. To protect filter coefficients from an adversary, efficient obfuscation techniques have been proposed, either by hiding them behind decoys or replacing them by key bits. In this article, we initially introduce a query attack that can discover the secret key of such obfuscated FIR filters, which could not be broken by existing prominent attacks. Then, we propose a first of its kind hybrid technique, including both hardware obfuscation and logic locking using a point function for the protection of parallel direct and transposed forms of digital FIR filters. Experimental results show that the hybrid protection technique can lead to FIR filters with higher security while maintaining the hardware complexity competitive or superior to those locked by prominent logic locking methods. It is also shown that the protected multiplier blocks and FIR filters are resilient to existing attacks. The results on different forms and realizations of FIR filters show that the parallel direct form FIR filter has a promising potential for a secure design.

Index Terms—hardware obfuscation, logic locking, oracle-less and oracle-guided attacks, constant multiplications, FIR filters, direct and transposed forms.

I. INTRODUCTION

Due to the increase in the design complexity of Integrated Circuits (ICs) and the rising costs of chip fabrication at advanced technology nodes, the IC supply chain has become heavily specialized and globalized [1]. Design houses have been combining their Intellectual Properties (IPs) with many others purchased from third-parties and resorting to *untrusted* foundries for fabrication. Although such globalization reduces the overall cost of producing an IC, it leads to serious security threats – especially for IPs – such as piracy, overuse, modification, and reverse engineering [2]. Over the years, IP protection has received a significant amount of interest and efficient methods, including watermarking [3], digital rights management [4], metering [5], and hardware obfuscation [6], have been introduced. Among these techniques, only hardware obfuscation can prevent IP theft, while the others are useful to prove the IP owner and reveal the IP owner’s rights during a litigation process. Hardware obfuscation aims to make the

design less clear and hard to understand for an adversary, by hiding the design content using structural transformations, locking the design functionality using additional logic with key bits, and exploiting camouflaged gates [6].

Digital filtering is frequently used in Digital Signal Processing (DSP) applications and Finite Impulse Response (FIR) filters are generally preferred due to their stability and linear phase property [7]. Since filter coefficients determine the filter behavior, they are actually an IP and need protection from reverse engineering by an adversary. Although there exist many efficient high-level and behavioral obfuscation methods proposed for protecting IPs [8]–[13], digital FIR filters require specialized obfuscation techniques, since they should behave according to their specifications, such as pass-band and stopband frequencies and ripples [14]. However, there exist only a limited number of techniques proposed to obfuscate DSP circuits and especially, digital filters [15]–[18]. The technique of [15] generates the desired filter and also its obfuscated versions, grouped in two categories as meaningful and unmeaningful in terms of filter behavior, using high-level transformations, and combines these realizations using a key-based finite state machine and a reconfigurator. To make the reverse engineering of coefficients harder for an end-user, adding input and output noises was proposed in [16]. Recently, we introduced a hardware obfuscation technique that hides the filter coefficients behind decoys [17], [18]. In [17], decoys can be selected based on their Hamming distance to reduce the hardware complexity or chosen randomly to increase the corruption at the filter output. Since an obfuscated FIR filter may still generate the desired behavior under a wrong key in [17], decoys are selected in such a way that the obfuscated filter presents the desired behavior only when the secret key is provided in [18]. To do so, the lower and upper bounds of each filter coefficient are found and decoys are selected beyond these bounds. In [17], [18], the folded design of an FIR filter is considered as a case study and its Time-Multiplexed Constant Multiplication (TMCM) block is obfuscated at Register-Transfer Level (RTL).

In this article, we initially introduce the query attack, which can discover the original filter coefficients hidden behind decoys [17], [18] or replaced by key bits [9]. Then, we propose a hybrid technique, which includes both hardware obfuscation and logic locking, for the protection of digital FIR filters. To do so, first, we describe a defense technique that obfuscates the multiplier blocks of parallel direct and transposed forms of an FIR filter, i.e., Constant Array Vector Multiplication (CAVM) and Multiple Constant Multiplication (MCM), respectively, using decoys. We also present their hardware-efficient realizations with and without multipliers. Second, we enhance this

This work has been partially conducted in the project “ICT programme” which was supported by the European Union through the European Social Fund. It was also partially supported by European Union’s Horizon 2020 research and innovation programme under grant agreement No 952252 (SAFEST) and by the project MOOSIC ANR-18-CE39-0005 of the French National Research Agency (ANR).

L. Aksoy, F. Almeida, J. Raik, and S. Pagliarini are with the Department of Computer Systems, Tallinn University of Technology, Tallinn, Estonia (e-mail: {levent.aksoy, felipe.almeida, jaan.raik, samuel.pagliarini}@taltech.ee.)

Q.-L. Nguyen, M.-L. Flottes, and S. Dupuis are with LIRMM, University of Montpellier, CNRS, Montpellier, France (e-mail: {quang-linh.nguyen, marie-lise.flottes, sophie.dupuis}@lirmm.fr)

obfuscation technique by locking the obfuscated design using a point function to make the protected design resilient to well-known attacks and by thwarting the query attack to determine the secret key. The hybrid protection technique works at RTL and can be easily adapted to any application including constant multiplications, such as image and video processing and neural networks. The main contributions of this article are as follows:

- Query attack developed for breaking designs generated by constant obfuscation techniques;
- Secure hybrid technique, consisting of hardware obfuscation and logic locking, developed for the protection of FIR filters with different forms and realizations;
- Comprehensive results on obfuscation and logic locking of FIR filters in terms of hardware complexity, attack resiliency, and filter behavior.

Experimental results clearly show that the proposed hybrid protection technique leads to FIR filter designs with higher security and competitive hardware complexity when compared to previously proposed hardware obfuscation and logic locking methods. As an interesting outcome of this work, we show that the parallel direct form filter has better resiliency properties than other FIR filter forms and realizations.

The remainder of this article is organized as follows: Section II presents background concepts. The query attack is described in Section III and the hybrid protection method is introduced in Section IV. Experimental results are presented in Section V. Further discussions on how other techniques may identify the original filter coefficients are given in Section VI. Finally, Section VII concludes the article.

II. BACKGROUND

This section initially presents frequently used notations and then, gives details on digital FIR filters and multiplierless constant multiplications. Finally, it summarizes related work.

A. Notations

Table I presents notations of important parameters used in the description of obfuscation and logic locking techniques.

TABLE I
SUMMARY OF NOTATIONS

c	Constant/filter coefficient
C	Constant array/set
n	Number of constants/filter coefficients
mbw	Maximum bit-width of constants/filter coefficients
X	Input variable/filter input
ibw	Bit-width of the input variable/filter input
Y	Output variable/filter output
k	Key bit
K	Secret key
p	Total number of key bits
v	Number of key bits for obfuscation
w	Number of key bits for logic locking

B. Digital FIR Filters

The FIR filter output $Y(j)$ is given as $\sum_{i=0}^{n-1} c_i \cdot X(j-i)$, where n is the filter length, c_i is the i^{th} filter coefficient, and $X(j-i)$ is the i^{th} previous filter input with $0 \leq i \leq n-1$. Fig. 1 shows the parallel and folded realizations of an FIR filter. Note that the filter output is obtained in a single clock

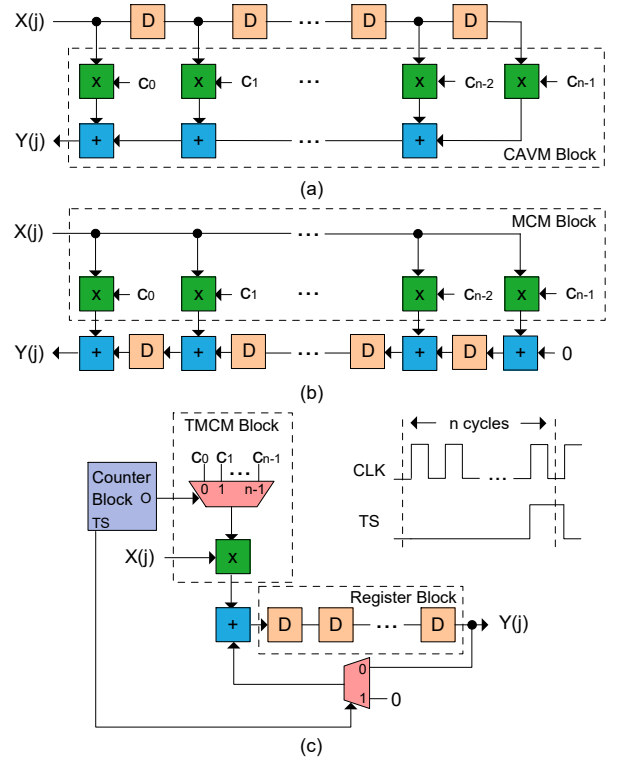


Fig. 1. Designs of an FIR filter: (a) parallel direct form; (b) parallel transposed form; (c) folded transposed form, where the counter counts from 0 to $n-1$. cycle in a parallel design, as shown in the direct and transposed forms in Figs. 1(a)-(b). On the other hand, the folded realization leads to a design with the least hardware complexity, since the common operations are re-used. However, it requires n clock cycles to compute the filter output, as shown in Fig. 1(c).

C. Multiplierless Design of Constant Multiplications

Multiplication of constant(s) by variable(s) is a ubiquitous and crucial operation in many DSP applications. Among others presented in [24], the CAVM, MCM, and TCMC blocks can be used in the design of a filter, as shown in Fig. 1. They are defined as follows:

- 1) The *CAVM operation* implements the multiplication of a $1 \times n$ constant array C by an $n \times 1$ input vector X , i.e., $Y = \sum_i c_i X_i$ with $1 \leq i \leq n$.
- 2) The *MCM operation* computes the multiplication of a set of n constants C by a single variable X , i.e., $Y_i = c_i X$ with $1 \leq i \leq n$.
- 3) The *TCMC operation* realizes the multiplication of a constant selected from a set of n constants C by a single variable X at a time, i.e., $Y = c_i X$ with $1 \leq i \leq n$.

Since the constants are determined beforehand, these constant multiplications can be realized using addition, subtraction, and shift operations under the shift-adds architecture. Note that parallel shifts can be implemented virtually for free in hardware using only wires. A straightforward shift-adds design technique, called the Digit-Based Recoding (DBR) [25], can realize constant multiplications in two steps: i) define the constants under a particular number representation, e.g., binary; ii) for the nonzero digits in the representation of constants, shift the input variables according to digit positions

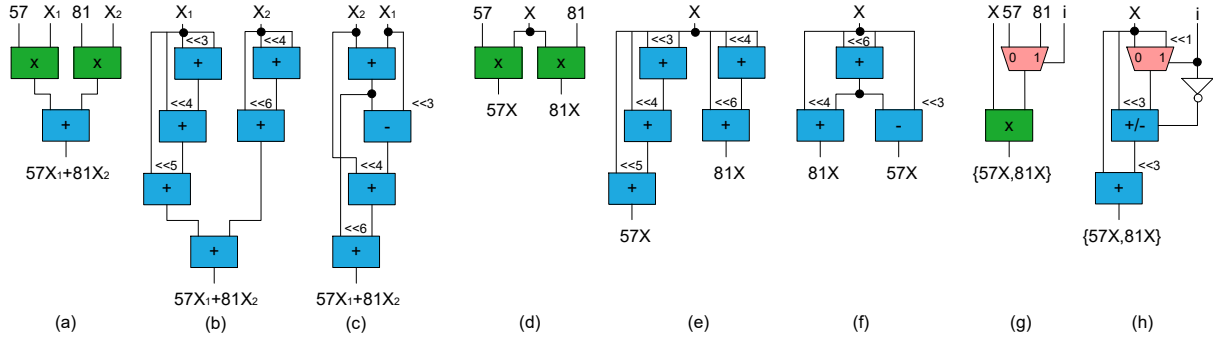


Fig. 2. Realizations of the CAVM (a-c), MCM (d-f), and TCM (g-h) blocks including constants 57 and 81: (a) using multipliers; (b) the DBR method [19]; (c) the method of [20]; (d) using multipliers; (e) the DBR method [19]; (f) the method of [21]; (g) using a multiplier; (h) the method of [22].

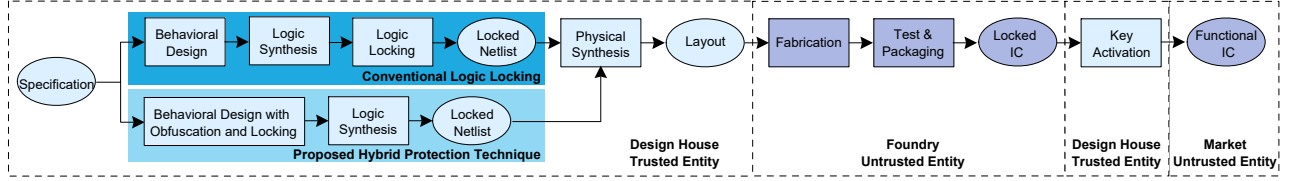


Fig. 3. Conventional logic locking and proposed hybrid protection technique in the IC design flow (adapted from [23]).

and add/subtract the shifted variables with respect to digit values. Furthermore, the number of operations can be reduced by maximizing the sharing of common subexpressions among constant multiplications [20]–[22], [26], [27].

As a simple example, consider the CAVM, MCM, and TCM blocks realizing constant multiplications, where C includes $57 = (111001)_{bin}$ and $81 = (1010001)_{bin}$. These constant multiplications are shown in Fig. 2. Note that the adder/subtractor shown in Fig. 2(h) behaves as an adder or a subtractor when its select input is 0 or 1, respectively. Observe from Figs. 2(b)-(c) and (e)-(f) that the sharing of common subexpressions can lead to a significant reduction under the shift-adds architecture in terms of the number of operations with respect to the DBR method.

D. Related Work

Hardware obfuscation can take place at different stages in the IC design flow, e.g., high-level synthesis [11], RTL [9], gate-level [28], and layout level [29]. In hardware obfuscation, locking the design functionality is a common practice. Fig. 3 presents conventional logic locking applied at gate-level in the IC design flow. Note that after the layout of the locked netlist is shipped to the foundry without revealing the secret key, the locked IC is produced and delivered back to the design house. Then, values of the secret key are stored in a tamper-proof memory and the functional IC is sent to the market.

1) *Defenses*: Earlier logic locking methods have been applied at gate-level. After the introduction of the concept of Random Logic Locking (RLL) using XOR/XNOR gates in [28], many works focused on different types of key logic, such as AND/OR, multiplexors (MUXes), and look-up tables, taking into account the hardware complexity of the locked circuit [30]. However, the satisfiability (SAT)-based attack [31] overcame all the defenses existing at that time. To thwart the SAT-based attack and its variants, circuits have been locked using a point function that forces these attacks to explore an

exponential number of queries [23], [32]–[36]. Moreover, the obfuscation of a locked design is considered in [37].

However, as mentioned in [8], at a higher level in the IC design flow, the selection of critical blocks of the design to be obfuscated gets easier, the exploration of tradeoffs between overhead and attack resiliency becomes more efficient, and the optimization of the obfuscated design is more effective. Recently, high-level and behavioral obfuscation techniques have been presented in [8]–[12]. Related to digital FIR filters including a large number of constants, filter coefficients are obfuscated by replacing their bits by key bits in [9], [11].

We note that our proposed hybrid protection technique works at one level higher than the gate-level, i.e., at RTL, as also shown in Fig. 3.

2) *Attacks*: In logic locking, there are generally two threat models, namely oracle-less (OL) and oracle-guided (OG). In the OL threat model, only the gate-level netlist of the locked circuit is available to an adversary. In the OG threat model, it is assumed that an adversary can also obtain the functional IC programmed with the secret key from the market and use it as an oracle to apply inputs and observe outputs. Hence, in this model, the adversary has both the netlist of the locked circuit and the functional IC.

Under the OL threat model, due to the limited information available to the adversary, patterns in the structure of the locked netlist are studied using statistical analysis, Automated Test Pattern Generation (ATPG), and machine learning [38]–[41]. Structural attacks, which identify and remove the logic inserted by a logic locking method, are proposed in [42]–[44].

Under the OG threat model, the ATPG-based attack of [45] leverages testing principles, such as justification and sensitization while finding the secret key. The SAT-based attack [31] iteratively finds Distinguishing Input Patterns (DIPs) that rule out wrong keys and achieves decryption as shown in Algorithm 1. It generates two locked circuits with the same inputs (X), but two different keys (K_1 and K_2) described in a Conjunctive Normal Form (CNF) formula in a SAT problem

Algorithm 1 The SAT-based attack [31]

Inputs: Locked circuit LC and *oracle*.
Output: Secret key K .

```

1:  $i := 1$  ▷ Number of iterations
2:  $F_1 = LC(X, K_1, Y_1) \wedge LC(X, K_2, Y_2)$ 
3: while  $\text{sat}[F_i \wedge (Y_1 \neq Y_2)]$  do
4:    $X_i^d := \text{sat\_assignment}_X[F_i \wedge (Y_1 \neq Y_2)]$ 
5:    $Y_i^d := \text{oracle}(X_i^d)$ 
6:    $F_{i+1} := F_i \wedge LC(X_i^d, K_1, Y_i^d) \wedge LC(X_i^d, K_2, Y_i^d)$ 
7:    $i := i + 1$ 
8:  $K := \text{sat\_assignment}_{K_1}(F_i)$ 

```

(line 2). Then, it finds a DIP, which generates different outputs on these circuits, using a SAT solver (line 4) and computes the output based on the found DIP using the oracle (line 5). It adds the Boolean equations including key bits into the SAT problem, which are obtained after inserting the values of these inputs and outputs into these circuits (line 6). This process is iterated until the SAT problem becomes unsatisfiable (line 3), meaning that there exists no DIP to distinguish wrong keys from the secret key. Finally, it determines the secret key as the one found in the last iteration (line 8).

In a similar fashion, the SAT-based attack of [46] eliminates at least 2 DIPs in a single iteration. A Satisfiability Modulo Theory (SMT) solver is used instead of a SAT solver, providing more flexibility while encoding the problem [47], [48]. The so-called approximate attack of [49] aims for approximate functional recovery. The SAT-based attack of [50] achieves sequential deobfuscation using dynamic simplifications of key conditions. The attack of [51] discovers the vulnerabilities of the SAT-resilient logic locking methods of [32], [33]. In [52], a generic framework is developed to attack compound locking techniques. A security diagnosis tool, which can evaluate the structural vulnerability of a design locked by a provably secure logic locking technique, is introduced in [53].

III. THE QUERY ATTACK

The SAT-based attack [31] presented in Algorithm 1 guarantees that the found values of **all** key bits are equal to those of the secret key. To do so, it may use a large number of queries that are required to eliminate all the wrong keys. On the other hand, our query attack proves that the found value of a **single** key bit is equal to that of the associated one in the secret key. To do so, it uses a small number of queries that make each key bit observable at a primary output. Hence, it slightly increases the SAT problem size when compared to the SAT-based attack. Thus, it can easily cope with circuits including a large number of gates and key bits [54] and logic structures, such as a multiplier and a tree of AND gates [31], which the SAT-based attack generally finds hard to handle. In this section, we initially describe the proposed query attack and then, present its results on obfuscated designs.

A. Description

Our proposed OG SAT-based query attack is described in Algorithm 2. It initially finds queries using two strategies (line 1). In the first one, an ATPG tool is used to find the test

Algorithm 2 The query attack

Inputs: Locked circuit LC and *oracle*.
Output: Proven values of the secret key K .

```

1:  $Q := \text{find\_queries}(LC)$ 
2:  $F = LC(X, K, Y)$ 
3: for  $i := 1$  to  $2p$  do
4:    $Y_i := \text{oracle}(Q_i)$ 
5:    $F := F \wedge LC(Q_i, K, Y_i)$ 
6:  $K := \text{sat\_assignment}_K(F)$ 
7: for  $i := 0$  to  $p - 1$  do
8:   if  $\text{unsat}[F \wedge \overline{K_i}]$  then
9:      $K_i = K_i$ 
10: for  $i := 0$  to  $p - 2$  do
11:   for  $j := i + 1$  to  $p - 1$  do
12:     if  $\text{undefined}(K_i) \ \& \ \text{undefined}(K_j)$  then
13:       if  $\text{unsat}[F \wedge (K_i \neq K_j)]$  then
14:          $K_i = K_j$ 
15:       else if  $\text{unsat}[F \wedge (K_i \neq \overline{K_j})]$  then
16:          $K_i = \overline{K_j}$ 

```

patterns for the stuck-at-fault of each key bit on the locked circuit and the values of the related primary inputs are stored as queries. The aim of this strategy is to find input patterns that can propagate each key bit to a primary output, making it observable. In the second one, queries are obtained randomly. The aim of this strategy is to find input patterns that may make multiple key bits observable at primary outputs. In our experiments, we generate a total of $2p$ queries, where p denotes the total number of key bits.

Then, the locked circuit is described in a CNF formula \mathbb{F} by expressing each gate in its CNF (line 2). For each query (lines 3-5), it is applied to the oracle and the values of primary outputs are obtained (line 4). Then, the related input and output values are assigned to the associated nets in the locked circuit, the constant values of these nets are propagated, and the Boolean equations including key bits are derived in a CNF formula and added into \mathbb{F} (line 5).

After all the queries are considered, the SAT problem \mathbb{F} is solved using a SAT solver and the values of key bits are determined (line 6). Note that the locked circuit with the found values of key bits behaves exactly the same as the oracle under the given queries, but not under all possible input values. Hence, the found key is not guaranteed to be the secret key.

However, the found value of a key bit can be proven correct by using the concept of *proof by contradiction*. To do so, for each key bit (lines 7-9), the complement of its found value is added into \mathbb{F} and the SAT solver is run. If there exists no solution to \mathbb{F} , i.e., the SAT problem is unsatisfiable, the value of the related key bit in the secret key is proven to be the one in the found solution.

As an example, consider the majority circuit in Fig. 4(a) and suppose that it is locked using XOR/XNOR gates as given in Fig. 4(b). Assume that a query is found as $x_1x_2x_3 = 000$ and thus, the value of its output y is obtained as 0 using the oracle. After propagating these values on the locked circuit, a Boolean equation $\overline{k_0} \vee k_1 = 0$, i.e., $k_0 \wedge \overline{k_1}$ in CNF, is obtained as shown in Fig. 4(c). In the SAT solution, the key bit values are found as $k_1k_0 = 01$. Note also that these are the proven key values since a SAT solver guarantees that there exists no

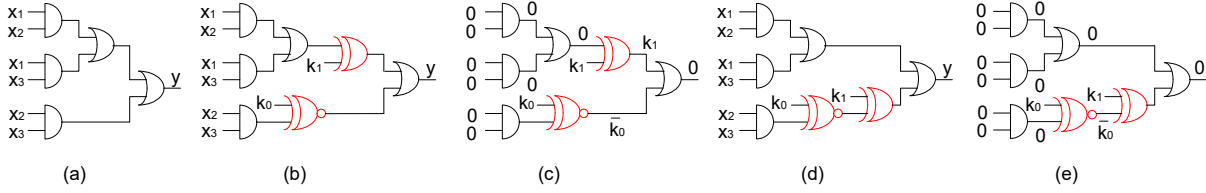


Fig. 4. Examples on the query attack: (a) majority circuit; (b)-(c) a locked majority circuit; (d)-(e) another locked majority circuit.

TABLE II
DETAILS ON FIR FILTERS AND THEIR TCMC BLOCKS.

Filter	Filter Details		TCMC Details	
	n	mbw	$\#in$	$\#out$
Mirzaei10a	71	15	39	47
LimYu07	121	14	39	46
Mirzaei10b	151	15	40	47

TABLE III
ATTACKS ON OBFUSCATED TCMC BLOCKS.

Filter	p	Architecture	Attacks			
			SAT		ATPG	
			time	time	prv	time
Mirzaei10a	128	TCMC-MUL [17]	OoT	OoT	128	212
		TCMC-CRK [9]	OoT	OoT	128	341
LimYu07	128	TCMC-MUL [17]	OoT	OoT	128	112
		TCMC-CRK [9]	OoT	OoT	128	365
Mirzaei10b	256	TCMC-MUL [17]	OoT	OoT	256	809
		TCMC-CRK [9]	OoT	OoT	256	852

solution to the SAT problem \mathbb{F} when it is extended by either the constraint $k_0 = 0$, i.e., $\overline{k_0}$ in CNF or $k_1 = 1$, i.e., k_1 in CNF, due to a conflict with the found Boolean equation, i.e., $k_0 \wedge \overline{k_1}$ in CNF.

We note that the query attack is also capable of proving if the value of a key bit, k_i , is equal to the value of another key bit, k_j , or its opposite (lines 10-16). To do so, we extend the SAT problem with $k_i \neq k_j$, i.e., $(k_i \vee k_j) \wedge (\overline{k_i} \vee \overline{k_j})$ in CNF, and $k_i = \overline{k_j}$, i.e., $(k_i \vee k_j) \wedge (\overline{k_i} \vee k_j)$ in CNF, respectively, where $i \neq j$ and $0 \leq i, j \leq p-1$. We run the SAT solver and check if the SAT problem is unsatisfiable. In this case, relations between two key bits are found independent of their values.

Returning back to our majority circuit, consider its another locked version given in Fig. 4(d). Assume that a query is again found as $x_1x_2x_3 = 000$ and hence, the output y is computed as 0. Thus, after the propagation of input and output values as shown in Fig. 4(e), a Boolean equation $\overline{k_0} \oplus k_1 = 0$, i.e., $(k_0 \vee k_1) \wedge (\overline{k_0} \vee \overline{k_1})$ in CNF, is found. In the SAT solution, the key bit values are found as $k_1k_0 = 10$. Although the actual values of key bits could not be proven, it is found that k_0 and k_1 have opposite values after the SAT problem is extended with the Boolean equation $k_0 \neq \overline{k_1}$ and it becomes unsatisfiable. Hence, the values of key bits $k_1k_0 = 10$ or $k_1k_0 = 01$ in the locked design lead to the original majority circuit.

B. Results

First, three FIR filters with a large number of coefficients and a large bit-width of filter input and coefficients were used to demonstrate the performance of the query attack. They were taken from [55]. Table II presents their details, where n and mbw are the number and maximum bit-width of coefficients, respectively. The folded realization of these filters was considered. Table II presents details on their TCMC blocks, where $\#in$ and $\#out$ are respectively their number of inputs and

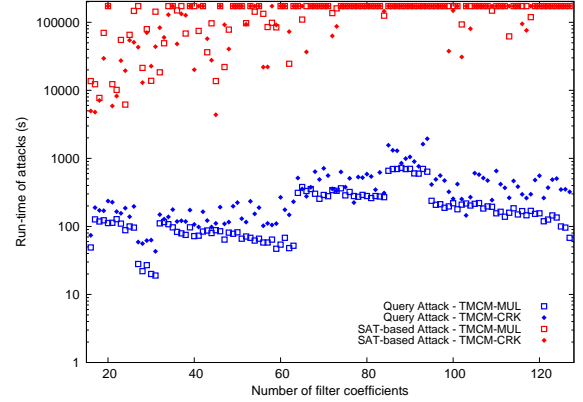


Fig. 5. Run-time of attacks on obfuscated TCMC blocks.

outputs when the bit-width of the input variable, i.e., ibw , is set to 32. These TCMC blocks were obfuscated using decoys under the architecture including MUXes and a multiplier [17], denoted as TCMC-MUL, and also obfuscated by replacing constants with key bits [9], denoted as TCMC-CRK.

Table III presents the number of key bits p and the results of the query attack along with the SAT- and ATPG-based attacks taken from [56]. In this table, $time$ denotes the run-time of an attack in seconds and prv stands for the number of key bits, whose values are proven by the query attack. Also, OoT indicates that an attack could not find a solution due to the time limit, which was set to 2 days. The attacks were run on a computing cluster including Intel Xeon processing units at 2.4 GHz with 40 cores and 96 GB memory. The query attack was developed in Perl and equipped with the ATPG tool Atalanta [57] and the SAT solver CaDiCaL [58]. It is available at <https://github.com/Centre-for-Hardware-Security/>.

Observe from Table III that the query attack can easily find the secret key of obfuscated designs while it is hard for the well-known attacks to find a solution. The main reason is that the TCMC block includes a multiplier block, where one of its inputs is the 32-bit input variable, and the SAT-based attack is not effective on designs including a multiplier as mentioned in [31]. However, the query attack can deal with a small number of queries, which are sufficient to determine the value of each key bit, using a little computational effort.

Second, we generated a total of 112 FIR filters, where n ranges between 16 and 127 when mbw was set to 12, to find the impact of the number of constants and key bits on the performance of the query attack. Again, the folded design of these filters were considered and ibw was set to 32. The TCMC blocks were obfuscated using $2^{\lfloor \log_2 n \rfloor + 1}$ key bits under the TCMC-MUL and TCMC-CRK architectures. The SAT-based [31] and query attacks were run on these obfuscated TCMC blocks, where the time limit was set to 2 days. Fig. 5 presents the run-time of these attacks.

Algorithm 3 Selection of decoys for original constants

Inputs: Original constants $C = \{c_1, c_2, \dots, c_n\}$ and v key bits.
Output: Decoy set D .

```

1:  $noi = 0$  ▷ Number of iterations
2:  $nok = 0$  ▷ Number of used key bits
3:  $D = \emptyset$  ▷ Set of  $n$  decoy constant arrays
4: while  $nok < v$  do
5:    $nod = 2^{noi}$  ▷ Number of decoys to be assigned
6:   for  $i = 1$  to  $n$  do
7:      $D_i = \text{AssignDecoy}(D_i, c_i, nod)$ 
8:      $nok = nok + 1$ 
9:     if  $nok == v$  then
10:      break
11:    $noi = noi + 1$ 

```

Observe from Fig. 5 that as n and p increase, the run-time of the query attack increases slightly. Note that while the query attack can find the secret key of each instance, the SAT-based attack can find a solution on 39 and 43 instances under the TMCM-MUL and TMCM-CRK architectures, respectively. Observe that the query attack runs faster than the SAT-based attack on these instances. Note that Section V presents more results of the query attack on different multiplier blocks obfuscated and locked by different techniques.

IV. PROPOSED HYBRID PROTECTION TECHNIQUE

This section initially presents the obfuscation technique used to hide filter coefficients behind decoys in the CAVM and MCM blocks of parallel direct and transposed forms of FIR filters (cf. Section IV-A and Section IV-B, respectively). Then, it describes the logic locking method using a point function described at RTL (cf. Section IV-C). Finally, it introduces the hybrid protection technique including both of these methods (cf. Section IV-D).

The original constants can be obfuscated using decoys as described in [17]. The motivation behind such obfuscation is that the use of decoys enables us to control the tradeoff between hardware complexity, output corruption, and filter behavior [17], [18] when compared to logic locking. The obfuscation technique using decoys requires two main steps: i) given the number of key bits, determine decoys for each original constant; ii) realize the obfuscated design, where original constants are hidden behind decoys using MUXes and key bits. The selection of decoys for the original constants is done as shown in Algorithm 3. In its *AssignDecoy* function (line 7), decoy selection can be done based on a given criterion, namely hardware complexity, output corruption, and filter behavior. In these criteria, decoys are chosen to be unique to increase the obfuscation.

A. Hardware Obfuscation of the CAVM Block

Given $1 \times n$ original constant array $C = [c_1, c_2, \dots, c_n]$ and the number of key bits for obfuscation, i.e., v , let D denote a set of n decoy constant arrays, i.e., $D = \{[d_1^1, \dots, d_1^{nd_1}], [d_2^1, \dots, d_2^{nd_2}], \dots, [d_n^1, \dots, d_n^{nd_n}]\}$, where nd_i is the number of decoy constants selected for the i^{th} original constant determined based on a given criterion with $1 \leq i \leq n$. Then, the set R , which includes each original

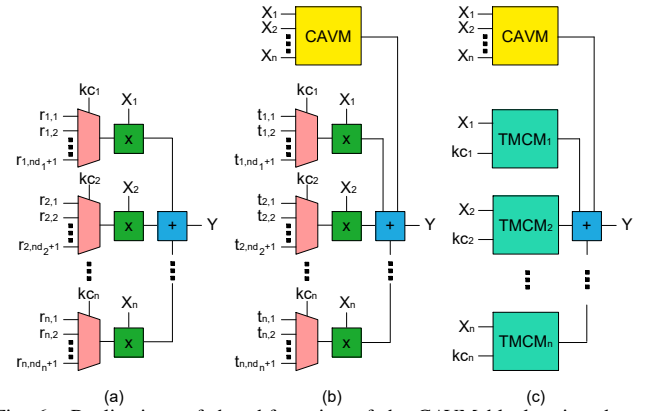


Fig. 6. Realizations of the obfuscation of the CAVM block using decoys: (a) straightforward design; (b) CAVM-MUL; (c) CAVM-SA.

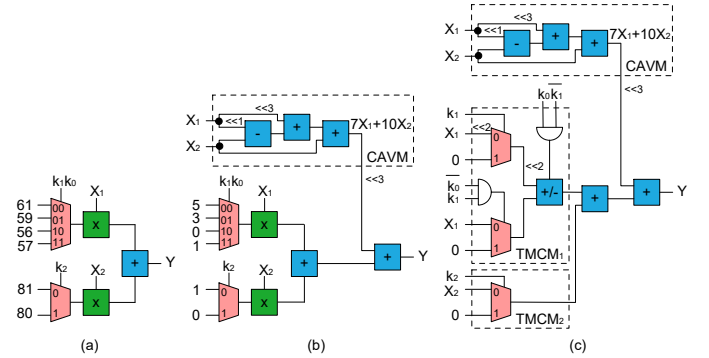


Fig. 7. Realizations of the obfuscation of the CAVM block including constants 57 and 81: (a) straightforward design; (b) CAVM-MUL; (c) CAVM-SA.

constant and its decoys, i.e., $R_i = c_i \cup D_i = [c_i, d_i^1, \dots, d_i^{nd_i}]$ with $1 \leq i \leq n$, is formed. Let $r_{i,j}$ denote the j^{th} constant in R_i with $1 \leq i \leq n$ and $1 \leq j \leq nd_i + 1$. Thus, the straightforward realization of the obfuscated CAVM block is given in Fig. 6(a). Note that the key bits determined for each constant, i.e., kc_i , have the size of $\lceil \log_2(nd_i + 1) \rceil$ with $1 \leq i \leq n$. The secret key, which is formed as the concatenation of these key bits, is determined based on the location of the original constant in the constant array R_i .

Note that the size of a multiplier given in Fig. 6(a) is related to the bit-width of the original constant and its decoy(s). Hence, to reduce the hardware complexity of the straightforward design, the size of constants, which are inputs of MUXes, can be decreased. To do so, we implement a CAVM block, where each entry of its constant array S is an element of each R array, i.e., $S = [s_1, s_2, \dots, s_n]$ with $s_i \in R_i = [c_i, d_i^1, \dots, d_i^{nd_i}]$ and $1 \leq i \leq n$. Then, the original constant and its decoys at inputs of each MUX are computed as $T_i = R_i - s_i$ with $1 \leq i \leq n$. Fig. 6(b) presents the obfuscated design under the proposed architecture called CAVM-MUL. Note that the CAVM block realizes $s_1 X_1 + s_2 X_2 + \dots + s_n X_n$ and is implemented under the shift-adds architecture using the algorithm of [20]. The constants to be in S are decided based on the hardware complexity of the CAVM block and the size of multipliers. This problem is formulated as a 0-1 Integer Linear Programming (ILP) problem.

To further reduce the hardware complexity of the design in Fig. 6(b), each multiplier with a MUX, which represents a TMCM block, is realized under the shift-adds architecture using the algorithm of [22]. Fig. 6(c) presents the obfuscated design under the proposed architecture called CAVM-SA.

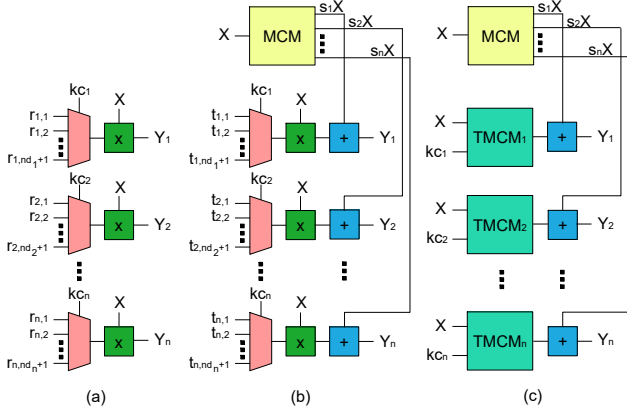


Fig. 8. Realizations of the obfuscation of the MCM block using decoys: (a) straightforward design; (b) MCM-MUL; (c) MCM-SA.

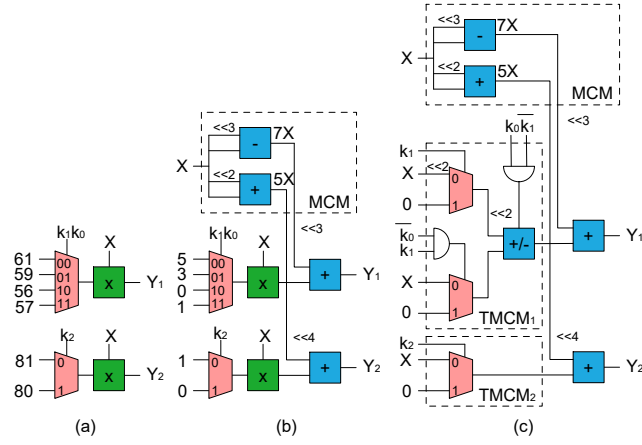


Fig. 9. Realizations of the obfuscation of the MCM block including constants 57 and 81: (a) straightforward design; (b) MCM-MUL; (c) MCM-SA.

Returning to our example in Fig. 2 with $C = [57, 81]$ and assuming that the number of key bits is 3, the set D , that includes decoys for each constant, is found as $D = \{\{61, 59, 56\}, [80]\}$ based on the hardware complexity criterion. Thus, the set R is formed as $R = \{\{61, 59, 56, 57\}, [81, 80]\}$. The straightforward realization of the obfuscated CAVM block using decoys is shown in Fig. 7(a), where the secret key is $\mathbf{K} = k_2k_1k_0 = 011$. Under the CAVM-MUL and CAVM-SA architectures, the constant array S is determined as $S = [56, 80]$. Thus, the set T is formed as $\{\{5, 3, 0, 1\}, [1, 0]\}$ leading to multipliers with smaller sizes when compared to those given in Fig. 7(a). The realization of the obfuscated CAVM design under the CAVM-MUL architecture is given in Fig. 7(b). Furthermore, Fig. 7(c) presents the shift-adds realization of the TCMC blocks implementing the constant multiplications including those in the set T under the CAVM-SA architecture.

In addition to the obfuscation using decoys on the CAVM block, we also developed the constant obfuscation technique used in the ASSURE tool [9]. Given the number of key bits, constants in the original CAVM block are replaced by key bits under the architecture called CAVM-CRK.

B. Hardware Obfuscation of the MCM Block

Similarly, the MCM block can also be obfuscated using decoys. After decoys selected for each original constant are found based on the given criterion, and the set R is determined,

$X_2 X_1 X_0$	$K^7 K^6 K^5 K^4$	K^3	$K^2 K^1 K^0$	$X_2 X_1 X_0$	$K^7 K^6 K^5 K^4$	K^3	$K^2 K^1 K^0$
0 0 0	0 0 0 0	0	0 0 1	0 0 0	0 0 0 0	0	0 0 1
0 0 1	0 0 0 0	0	0 1 0	0 0 1	0 0 0 0	0	0 0 1 1
0 1 0	0 0 0 0	0	1 0 0	0 1 0	0 0 0 0	0	0 1 1 0
0 1 1	0 0 0 0	0	0 0 0	0 1 1	0 0 0 0	0	0 1 0 0
1 0 0	0 0 0 1	0	0 0 0	1 0 0	0 0 0 1	0	0 0 0 0
1 0 1	0 0 1 0	0	0 0 0	1 0 1	0 0 1 1	0	0 0 0 0
1 1 0	0 1 0 0	0	0 0 0	1 1 0	0 1 1 0	0	0 0 0 0
1 1 1	1 0 0 0	0	0 0 0	1 1 1	1 1 0 0	0	0 0 0 0

Fig. 10. (a) Behavior of a Boolean function locked by one-point function; (b) behavior of a Boolean function locked by relaxed one-point function.

the straightforward realization of the obfuscated design can be obtained as illustrated in Fig. 8(a). Moreover, the size of multipliers can be reduced by determining the set of constants S from the set R and the set T is computed accordingly as described in Section IV-A. The multiplications of constants in the set S by the variable X , i.e., s_1X, s_2X, \dots, s_nX , are realized in an MCM block, which is implemented under the shift-adds architecture using the algorithm of [21]. Fig. 8(b) presents the obfuscated design under the proposed architecture called MCM-MUL. Furthermore, the multiplierless realization of the design obfuscated under the MCM-MUL architecture can be obtained by realizing the TCMC block under the shift-adds architecture using the algorithm of [22]. Fig. 8(c) shows the obfuscated design under the proposed architecture called MCM-SA.

Returning to our example, Fig. 9 presents the straightforward realization of the obfuscated MCM block and its designs under the MCM-MUL and MCM-SA architectures.

In addition to the obfuscation using decoys, constants in the original MCM block are replaced by key bits under the architecture called MCM-CRK.

C. Logic Locking with a Point Function

As shown in Sections III and V, the constant obfuscation techniques are vulnerable to the SAT-based attack and its variants. The motivation behind locking the obfuscated design with a point function is to make it resilient to these techniques. In order to increase the number of DIPs to be explored in a SAT-based attack, one can lock primary outputs of a multiplier block using a point function¹ at RTL as done at gate-level in [23], [32]–[34].

Suppose that a Boolean function $f : \mathbb{B}^q \rightarrow \mathbb{B}$ is locked using a one-point function with w key bits, where $w \leq q$, leading to a locked Boolean function $g : \mathbb{B}^{w+q} \rightarrow \mathbb{B}$ and let \mathbf{K} denotes the secret key. Then, $f(X) = g(X, \mathbf{K})$ under all possible input values. Fig. 10(a) shows the behavior of the locked function g under each possible key value when $q = w = 3$ and $k_2k_1k_0 = 011$ is the secret key. In this figure, K^i stands for the assignment of the value i in binary to key bits, i.e., $k_{w-1} \dots k_1k_0 = (i)_{bin}$ with $0 \leq i \leq 2^w - 1$. Also, the value of logic 0 (1) under each possible key value denotes that the locked function g is (not) equal to the original function f . Note that the locked function under the secret key, i.e., $\mathbf{K} = K^3$ highlighted in our example, always generates the

¹A one-point function is a Boolean function that evaluates to 1 at exactly one input pattern.

```

// One-point function at RTL
always @(*) begin
  if (X == K)
    if (K == K)
      g = f;
    else
      g = !f;
  else
    g = f;
end
//Relaxed one-point function at RTL
always @(*) begin
  if ((X - K) >= q'd0 && (X - K) <= q'dcv)
    if (K == K)
      g = f;
    else
      g = !f;
  else
    g = f;
end

```

Listing 1. Logic locking using a point function at RTL.

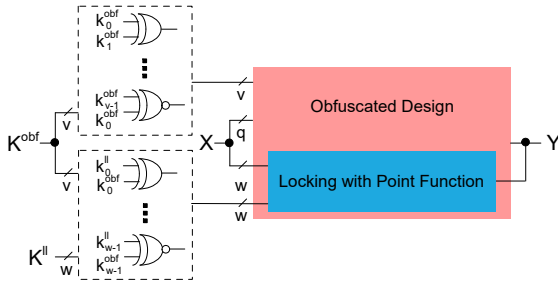


Fig. 11. Proposed hybrid protection technique.

same output as the original function for every input pattern. Observe from Fig. 10(a) that each input pattern eliminates at most one wrong key, leading to an exponential number of DIPs to find the secret key, i.e., 2^w . Moreover, such a one-point function can be relaxed to increase the corruption at a primary output. For example, Fig. 10(b) presents the behavior of the locked function g , where each input pattern can eliminate at most 2 wrong keys. Observe that the exponential number of tries to find the secret key is still valid, i.e., 2^{w-1} in this case. Furthermore, multiple primary outputs can be locked using point functions with different key bits.

Listing 1 presents the Verilog code snippet, which describes logic locking using the one-point function at RTL. In this code, X is an array of primary inputs and K is an equally sized array of key bits. Moreover, the relaxed one-point function can also be described at RTL as shown in the same listing. In its code, cv stands for the corruption value, which denotes the maximum number of wrong keys that can be distinguished by a single input pattern.

We note that since the point function is described at RTL, the synthesis tool shapes its circuit based on the given synthesis parameters. Thus, its realization does not have a regular structure like logic locking methods of [33], [34], [36].

D. Combination of Obfuscation and Logic Locking

The hybrid protection technique includes obfuscation and logic locking using a point function described in previous subsections. Initially, the obfuscation technique using decoys is applied and then, the obfuscated design is locked using a point

TABLE IV
DETAILS ON THE FIR FILTER AND ITS MULTIPLIER BLOCKS.

Filter	n	mbw	Multiplier Block	#in	#out
Johansson08	30	10	CAVM	480	31
			MCM	16	733
			TCMC	21	26

function. Fig. 11 illustrates the hybrid protection technique, where X and Y denote the inputs and outputs of the original design and K^{obf} and K^{ll} stand for the key bits used for obfuscation and locking, respectively. Additionally, to thwart the structural attacks, the key bits used for logic locking, K^{ll} , are hidden among the key bits used for obfuscation, K^{obf} , using XOR/XNOR gates. In this scheme, an XOR (XNOR) gate, which has k_i^{ll} and k_j^{obf} as inputs, is generated if the value of k_j^{obf} in the secret key is equal to logic 0 (1) value, where $0 \leq i \leq w-1$ and $0 \leq j \leq v-1$. Then, the output of this gate is connected to the net, which would be driven by k_i^{ll} . Moreover, to thwart the query attack, each k_i^{obf} is hidden among another k_j^{obf} using an XOR/XNOR gate, where $i \neq j$ and $0 \leq i, j \leq v-1$. By doing so, each key bit is observed with other key bits at a primary output, making it harder for the query attack to prove the value of the related key bit.

We developed a Computer-Aided Design (CAD) tool to automate the design and verification process for the obfuscation and locking of the CAVM, MCM, and TCMC blocks and the parallel direct and transposed form and folded FIR filters. The CAD tool takes the filter coefficients, the number of key bits, the design architecture, and other design parameters as inputs and generates the description of the obfuscated design in Verilog, the testbench for verification, and synthesis and simulation scripts. Note that designs are described in a behavioral fashion at RTL.

V. EXPERIMENTAL RESULTS

In this section, we introduce the gate-level synthesis results of multiplier blocks protected by the proposed hybrid technique, obfuscated by previously proposed techniques, and locked by prominent logic locking methods. We also provide the results of well-known logic locking attacks and the proposed query attack on these designs. Furthermore, we present the results of obfuscated and locked FIR filters and also, introduce the results of prominent attacks on these designs. Finally, we explore the impact of parameters used in the point function on the hardware complexity and resiliency to the SAT-based attack and present gate-level synthesis results of the obfuscated and locked CAVM block of the direct form filter, which has promising security properties.

A. Results of Obfuscated and Locked Multiplier Blocks

Based on our experimental observations, similar outcomes have been observed on FIR filters with a different number of coefficients and different bit-width of filter input and coefficients in comparison of design architectures, obfuscation and locking techniques, and attacks. Hence, in this experiment, a single FIR filter with a small number of coefficients and a small bit-width of filter input and coefficients was used to reveal the effectiveness of obfuscation and locking techniques.

TABLE V
RESULTS OF OBFUSCATED AND PROTECTED MULTIPLIER BLOCKS.

Block	Architecture	Technique	Synthesis			Attacks								
						SAT	ATPG	AppSAT	DoubleDIP	Query		SCOPE		
			area	delay	power	time	time	time	time	prv	time	cdk/dk	time	
CAVM	CAVM-MUL	Decoy [17]	15435	4616	4641	155143	OoT	OoT	OoT	OoT	32	9893	20/32	8
		Proposed Hybrid	15710	4611	4757	OoT	OoT	OoT	OoT	0	OoT	1/1	13	
	CAVM-SA	Decoy [17]	15465	4611	4475	36083	4539	OoT	OoT	32	9944	20/32	8	
		Proposed Hybrid	15704	4715	4497	OoT	OoT	OoT	OoT	0	29328	1/1	12	
	CAVM-CRK	Constant [9]	18737	3982	4756	110	1446	OoT	OoT	32	897	21/27	11	
		Proposed Hybrid	18976	4265	4809	OoT	OoT	OoT	OoT	0	1937	2/3	16	
MCM	MCM-MUL	Decoy [17]	10949	3102	2839	106	OoT	324	243	32	176	27/32	7	
		Proposed Hybrid	11173	3031	2897	OoT	OoT	OoT	OoT	0	197	1/1	11	
	MCM-SA	Decoy [17]	10493	3112	2493	119	OoT	342	254	32	152	27/32	7	
		Proposed Hybrid	10705	3159	2495	OoT	OoT	OoT	OoT	0	115	1/1	11	
	MCM-CRK	Constant [9]	12799	2772	2412	159	OoT	415	300	32	459	18/32	7	
		Proposed Hybrid	13038	2970	2456	OoT	OoT	OoT	OoT	0	759	1/1	11	
TMCM	TMCM-MUL	Decoy [17]	1545	3517	610	241	6783	378	496	32	7	21/32	4	
		Proposed Hybrid	1794	4278	639	OoT	OoT	OoT	OoT	0	17	2/3	2	
	TMCM-SA	Decoy [17]	2043	4452	1037	738	963	935	OoT	32	37	17/32	4	
		Proposed Hybrid	2245	4536	1065	OoT	OoT	OoT	OoT	0	42	1/2	3	
	TMCM-CRK	Constant [9]	1566	2997	623	1035	15571	1032	OoT	32	29	20/32	4	
		Proposed Hybrid	1776	3655	642	OoT	OoT	OoT	OoT	0	48	1/1	2	

TABLE VI
RESULTS OF LOCKED MULTIPLIER BLOCKS.

Block	Logic Locking	Synthesis			Attacks							
					SAT	ATPG	AppSAT	DoubleDIP	Query		SCOPE	
		area	delay	power	time	time	time	time	prv	time	cdk/dk	time
CAVM	RLL	16411	3385	4183	171	OoT	205	2609	32	254	0/0	9
	RLL+AntiSAT	16492	3416	4127	OoT	OoT	OoT	OoT	16	364	0/0	14
	RLL+CASLock	16473	3502	4110	OoT	OoT	OoT	OoT	16	443	0/0	13
	RLL+SARLock	16512	3572	4191	OoT	OoT	48855	OoT	32	441	8/8	13
	RLL+SFLL	16506	3473	4205	339	829	39664	OoT	32	436	0/0	14
	RLL+SKGLock	16559	3894	4308	OoT	OoT	OoT	OoT	19	513	5/6	14
MCM	RLL	8090	2398	2039	86	122	293	371	32	89	0/0	6
	RLL+AntiSAT	8244	2434	2065	OoT	OoT	OoT	OoT	16	249	0/0	9
	RLL+CASLock	8121	2404	2024	OoT	OoT	1054	OoT	16	164	0/0	9
	RLL+SARLock	8209	2467	2041	OoT	OoT	45013	OoT	32	228	10/10	9
	RLL+SFLL	8166	2452	2019	576	7870	2626	OoT	32	243	0/0	9
	RLL+SKGLock	8252	2464	2056	OoT	OoT	OoT	OoT	19	160	5/5	9
TMCM	RLL	1587	3712	646	8	39	57	77	32	15	0/0	2
	RLL+AntiSAT	1659	3545	632	OoT	OoT	OoT	OoT	13	28	0/0	2
	RLL+CASLock	1653	3664	628	OoT	OoT	OoT	OoT	15	20	0/0	2
	RLL+SARLock	1659	3756	658	OoT	OoT	2662	OoT	31	36	6/6	3
	RLL+SFLL	1644	3800	653	1095	1089	5363	OoT	32	36	0/0	2
	RLL+SKGLock	1694	3739	676	OoT	OoT	OoT	OoT	18	34	10/10	2

Table IV presents the details of this filter taken from [55], where $\#in$ and $\#out$ are respectively the number of inputs and outputs of the multiplier blocks when ibw is 16.

Table V presents the synthesis results of the CAVM, MCM, and TMCM blocks of the FIR filter obfuscated by previously proposed methods [9], [17] and protected by the proposed hybrid technique. Note that the TMCM-SA architecture denotes the TMCM block obfuscated using decoys under the shift-adds architecture. Logic synthesis was performed by Cadence Genus using a commercial 65 nm cell library with the aim of area optimization. For this aim, a very high virtual clock period value, i.e., 80 ns, was used. The encrypted designs were validated by simulation using 10,000 randomly generated inputs, where the switching activity data of each node in the design were collected and stored in a Switching Activity Interchange Format (SAIF) file, which is later used by the synthesis tool while computing the power dissipation. For obfuscation, 32 key bits were used. There were 16 key bits for locking using the one-point function. Thus, a total of 48 key bits were used in designs protected by the hybrid technique. In this table, *area*, *delay*, and *power* stand for the total area

in μm^2 , delay in the critical path in ps , and total power dissipation in μW , respectively. This table also presents the results of OG attacks, namely SAT- and ATPG-based attacks, the approximate AppSAT attack taken from [56], and the DoubleDIP attack taken from [59], and the OL SCOPE attack taken from [60]. For the SCOPE attack, *cdk* and *dk* denote the number of correctly deciphered key bits and the number of deciphered key bits, respectively. The time limit given to the attacks was 2 days. In this table, designs, whose secret key has not been discovered by the given attacks, are highlighted.

1) *Comments on Hardware Complexity*: Observe from Table V that the hybrid protection technique increases the hardware complexity when compared to the obfuscation techniques simply due to the inclusion of the point function and logic for the obfuscation of key bits. Note that the increase of area in the CAVM, MCM, and TMCM blocks reaches up to 1.7%, 2%, and 13.8%, respectively. The obfuscation and hybrid protection of the CAVM and MCM blocks under the proposed architectures, i.e., CAVM-MUL, CAVM-SA, MCM-MUL, and MCM-SA, lead to designs with less area when compared to those realized under the CAVM-CRK and MCM-CRK archi-

TABLE VII
RESULTS OF OBFUSCATED AND LOCKED FIR FILTERS.

Filter	Obfuscation and Hybrid Protection							Logic Locking							
	Architecture	Technique	Synthesis			Attacks		Technique	Synthesis			Attacks			
						KC2	SCOPE					KC2	SCOPE		
			area	delay	power	time	cdk/dk		time	area	delay	power	time	cdk/dk	time
Direct	CAVM-MUL	Decoy [17]	19238	4907	3088	Failed	18/32	8	RLL	20233	3566	2906	Failed	15/18	10
		Proposed Hybrid	19500	4828	3153	OoT	1/1	13	RLL+AntiSAT	20300	3512	2896	Failed	21/26	14
	CAVM-SA	Decoy [17]	19243	4792	3012	Failed	19/32	8	RLL+CASLock	20324	3746	2928	OoT	11/15	14
		Proposed Hybrid	19485	4798	3040	OoT	1/1	13	RLL+SARLock	20326	3630	2936	OoT	31/37	14
	CAVM-CRK	Constant [9]	22551	4228	2734	Failed	14/32	10	RLL+SFLL	20307	3619	2892	Failed	21/28	14
		Proposed Hybrid	22796	4244	2757	OoT	2/4	15	RLL+SKGLock	20380	4052	2994	Failed	16/24	15
Trans.	MCM-MUL	Decoy [17]	25195	3470	3848	100347	25/32	11	RLL	22362	3093	3303	67811	16/21	9
		Proposed Hybrid	25439	3540	3896	OoT	1/1	16	RLL+AntiSAT	22510	3218	3302	OoT	15/24	15
	MCM-SA	Decoy [17]	24967	3322	3569	82952	26/32	10	RLL+CASLock	22461	3337	3320	OoT	7/8	14
		Proposed Hybrid	25139	3346	3562	OoT	1/1	15	RLL+SARLock	22425	3183	3303	OoT	31/41	14
	MCM-CRK	Constant [9]	27126	3240	3273	51973	21/32	11	RLL+SFLL	22389	3116	3311	OoT	19/29	14
		Proposed Hybrid	27433	3256	3290	OoT	1/1	17	RLL+SKGLock	22514	3186	3329	OoT	17/24	15
Folded	TMCM-MUL	Decoy [17]	9126	4785	869	7478	20/32	2	RLL	9183	4496	904	7845	15/18	3
		Proposed Hybrid	9379	4665	933	OoT	2/2	3	RLL+AntiSAT	9225	4681	882	OoT	8/15	4
	TMCM-SA	Decoy [17]	9791	5758	1168	11895	18/32	2	RLL+CASLock	9237	4675	926	OoT	8/13	4
		Proposed Hybrid	9966	5646	1236	OoT	9/13	3	RLL+SARLock	9235	4761	911	OoT	31/31	4
	TMCM-CRK	Constant [9]	9126	4328	870	5657	22/32	2	RLL+SFLL	9222	4570	892	OoT	16/20	4
		Proposed Hybrid	9356	4602	894	OoT	1/1	3	RLL+SKGLock	9288	4434	910	OoT	18/31	4

tures. Note that such a decrease reaches up to 17.6% and 18% in the CAVM and MCM blocks, respectively. This is simply because the proposed techniques exploit common subexpressions shared in constant multiplications. On the other hand, the obfuscation and hybrid protection of the TMCM blocks under the TMCM-MUL and TMCM-CRK architectures lead to designs with less area with respect to those realized under the TMCM-SA architecture. Note that such a decrease reaches up to 24.3%. This is because a single multiplier is replaced by a large number of addition and subtraction operations under the TMCM-SA architecture. It is also observed that the minimum achievable delay values in the critical path of obfuscated and protected multiplier blocks are very close to each other, meaning that the inclusion of the point function and logic for the obfuscation of key bits does not have a significant impact while realizing the design with the smallest delay.

2) *Comments on Attack Resiliency*: Observe also from Table V that while the OG attacks can easily discover the secret key on the obfuscated designs, the OL attack can decipher all the key bits with high accuracy, except for the CAVM design obfuscated under the CAVM-CRK architecture. On the other hand, none of these attacks can break the defense built by the hybrid protection technique. Note that the designs protected by the hybrid technique were also applied to Fa-SAT [52] and the Valkyrie tool [53], but without any success due to the combination of both obfuscation and locking.

Moreover, these multiplier blocks under an architecture including a multiplier are locked by prominent logic locking methods, namely, RLL [28] and the SAT-resilient methods of AntiSAT [33], SARLock [32], SFLL [23], CASLock [34], and SKGLock [36]. In this case, the multiplier block described at RTL is initially synthesized and its gate-level netlist is obtained, and then, this netlist is locked. Note that while the RLL, AntiSAT, and SFLL methods were applied using the NEOS tool [61], the script for the SARLock method was provided by P. Subramanian, and we implemented the CASLock and SKGLock methods. In the RLL method, 32 key bits are used, the same as the obfuscation techniques presented

in Table V. Same as the hybrid protection method shown in Table V, there are a total of 48 key bits in the combination of RLL and a SAT-resilient method, while 16 key bits are designated to a SAT-resilient method. Note that due to the locking nature of AntiSAT, CASLock, and SKGLock, they require twice the number of designated key bits. Hence, a total of 32 key bits are used in these methods. Table VI presents the results of locked multiplier blocks. The locked designs, whose secret key has not been discovered by the given attacks, are also highlighted.

3) *Comments on Hardware Complexity*: Observe from Table VI that SAT-resilient methods with a combination of RLL lead to designs with hardware complexity very close to each other. When compared to the results of the hybrid protection technique given in Table V under the architectures using multiplier(s), the locked CAVM and MCM blocks have larger and smaller area, respectively and the locked TMCM blocks have competitive area. A locked MCM block has less hardware complexity than an obfuscated or protected MCM block because the logic locking is applied after the common subexpressions are exploited by the synthesis tool.

4) *Comments on Attack Resiliency*: Also, observe from Table VI that the secret key of designs locked by RLL, RLL+SARLock, and RLL+SFLL² can be found by the given attacks. Note also that the MCM block locked by RLL+CASLock could be broken by the AppSAT. While the query attack is also capable of proving the values of most of the RLL key bits in all logic locking methods and extra SKGLock key bits, the SCOPE attack can predict the values of some key bits of designs locked by RLL+SARLock and RLL+SKGLock with high accuracy.

B. Results of the Obfuscated and Locked FIR Filters

Table VII presents the synthesis results of parallel direct and transposed form and folded FIR filters, whose CAVM, MCM,

²Confirmed by the developer of the SFLL method that when a small number of key bits are used and their values are biased towards all logic 0s or 1s in the SFLL method, the exponential growth in the number of iterations in the SAT-based attack is no longer valid.

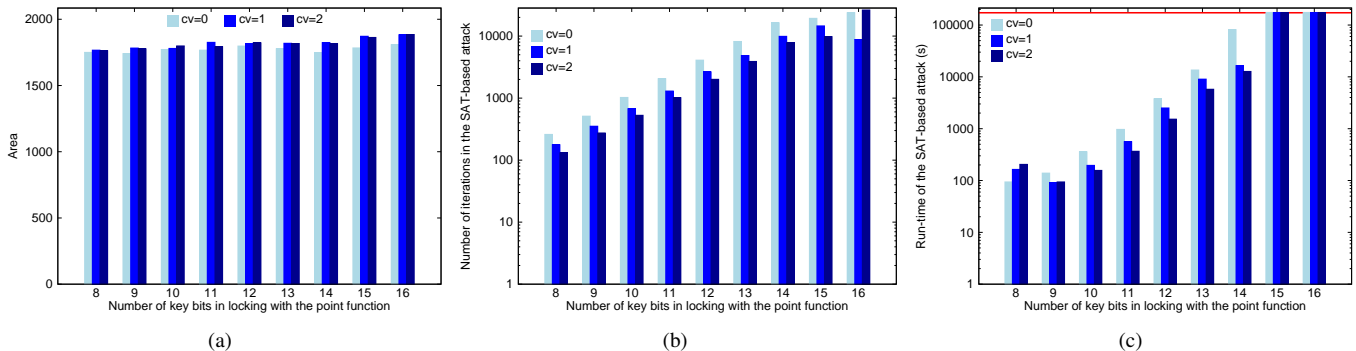


Fig. 12. Impact of point function parameters: (a) area; (b) number of iterations; (c) run-time.

and TCMC blocks are obfuscated by the previously proposed techniques [9], [17] and the hybrid protection technique, respectively. It also shows the synthesis results of FIR filters locked by prominent logic locking methods. It introduces the results of attacks that can be applied to sequential circuits namely, the OG KC2 attack, which was taken from [61], and the OL SCOPE attack. In this table, *failed* denotes that the found solution of the KC2 attack is actually a wrong key verified through simulation.

1) *Comments on Hardware Complexity:* Observe from Table VII that the direct form filter has less area and consumes less power, but has a higher delay when compared to the transposed form filter. On the other hand, the folded design has the smallest area, but the filter output is computed in 30 clock cycles, increasing the latency and energy consumption. The conclusions drawn based on the gate-level synthesis results on the obfuscated and locked multipliers blocks given in Tables V-VI are also valid on the obfuscated and locked FIR filters. However, due to the registers in the FIR design, the overhead on the overall FIR filter design gets smaller. Note that the proposed hybrid technique achieves the maximum area reduction with respect to the logic locking methods on the parallel direct form FIR filters, i.e., 4.4%, obtained when the FIR filter under the CAVM-SA architecture is compared to the FIR filter locked by RLL+SKGLock.

2) *Comments on Attack Resiliency:* Observe also from Table VII that the KC2 attack is capable of discovering the secret key of the obfuscated FIR filters using previously proposed techniques, except for the direct form filters, but it is not successful on the FIR filters protected by the proposed hybrid technique. It can also find the secret key locked by RLL, except for the direct form filter, but fails on the filters locked by both RLL and a SAT-resilient method. Similarly, the SCOPE attack generally deciphers all the key bits on the obfuscated FIR filters with high accuracy, but it can only decipher a small number of key bits of the FIR filters protected by the hybrid technique. However, it is capable of deciphering more key bits on the locked FIR filters when compared to its results on the locked multiplier blocks. This is heavily due to the resynthesis of the FIR filter including the locked multiplier block. Note that the proposed hybrid technique increases the area and power dissipation of FIR filters when compared to the previously proposed obfuscation techniques [9], [17] in order to increase their resiliency to the existing attacks.

C. Analysis on the Point Function

To find the impact of the point function and its parameters in the hybrid protection technique on the hardware complexity, the number of iterations taken in the SAT-based attack [31], and the run-time of the SAT-based attack [31], we used the TCMC block of our FIR filter under the TCMC-MUL architecture. Again, the TCMC block is obfuscated using decoys with 32 key bits when ibw is 16. In logic locking with the point function, the number of key bits, i.e., w , is determined to be between 8 and 16, the corruption value, i.e., cv , is set to be between 0 and 2, and a single primary output is locked. Fig. 12 presents the impact of point function parameters on the area of the protected TCMC block and the number of iterations and run-time of the SAT-based attack.

Observe from Fig. 12(a) that as the number of key bits used in logic locking, w , increases, the area of the protected TCMC block using the hybrid technique increases slightly. Note that as the corruption value, cv , increases, the design area increases simply due to the increased range of comparator logic given in Listing 1. Also, observe from Figs. 12(b)-(c) that as w increases, the number of iterations and run-time of the SAT-based attack increases. An exponential growth in the number of iterations and run-time can be observed till w is 15. As can be seen from Fig. 12(c), for the 15- and 16-bit keys in the point function, the SAT-based attack cannot find the secret key in the time limit, i.e., 2 days, denoted by the red line. Thus, the number of iterations given in Fig. 12(b) for these number of key bits, is the one obtained in the time limit. Note also that in all TCMC designs locked by the point function with the given parameters, the number of iterations increases exponentially, while it decreases as cv is increased, but still keeping the exponential growth.

To find the impact of locking an obfuscated design using a point function on hardware complexity and attack resiliency, we used the same 112 FIR filters presented in Section III-B, where n ranges between 16 and 127. In our experiments, the TCMC blocks of folded FIR filters were obfuscated using $2^{\lfloor \log_2 n \rfloor + 1}$ key bits under the TCMC-MUL architecture when ibw was set to 16. For the point function, 16 key bits were used. Fig. 13 presents the run-time of the SAT-based attack on obfuscated and protected TCMC blocks when its time limit was 2 days.

Observe from Fig. 13 that locking an obfuscated design using a point function increases the SAT-based attack resiliency

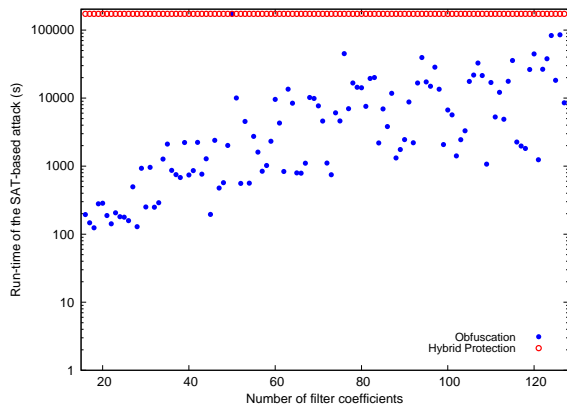


Fig. 13. Run-time of the SAT-based attack on TCMC blocks.

TABLE VIII
DETAILS ON THE PROTECTED AND LOCKED CAVM BLOCKS.

Filter	n	mbw	p	Hybrid			RLL+CASLock		
				area	delay	power	area	delay	power
Dempster02	25	12	41	11145	5903	7057	16557	3136	4238
Johansson08	30	10	46	14826	4662	4504	16461	3381	4101
Shi11_Y2	34	11	50	12270	3594	3567	12533	3163	3190
Shi11_A	59	10	75	21431	4858	5825	20993	3404	5390
Samueli89	60	13	76	24188	4130	7522	26696	3998	6819
Lim83	63	10	79	22932	4848	6652	24696	3661	6322
Yoshino09	64	13	80	25096	4964	7927	30414	3437	7927
Nielsen89	67	15	83	26187	5318	9645	34950	4071	9164
Maskell07	108	9	124	37306	4811	9049	37148	3604	9522
LimYu07	121	14	137	48354	4947	16862	59492	3888	15346

significantly. Note that the SAT-based attack can find a solution to all obfuscated TCMC blocks except one. However, the average area, delay, and power dissipation of the protected designs are increased by 10.7%, 7.1%, and 9.6%, respectively when compared to those of the obfuscated designs.

D. Analysis on the Direct Form FIR Filter

Among the parallel design of FIR filters, the direct form is a good candidate to be used in a secure implementation for several reasons based on the results obtained in this work. First, as shown in Table VII, its obfuscated hardware complexity in terms of area and power dissipation is significantly smaller than the transposed form filter. Second, it includes a large number of multiplication operations in chain, which make the SAT-based attack and its variants hard to discover the secret key. Third, the CAVM block of the direct form filter has a large number of inputs than the MCM block of the transposed form filter, which enables an increase in the number of key bits in the point function, improving the resiliency of the design protected by the hybrid technique as shown in Figs. 12(b)-(c). This last observation is also true when compared to the TCMC block used in folded FIR filter design.

To find the impact of the number of coefficients on the hardware complexity of the protected CAVM block of an FIR filter, 10 filters were taken from [55], where n ranges between 25 and 121 and mbw is between 9 and 15. In the design of CAVM blocks, ibw is set to 16. In the hybrid protection technique, these CAVM blocks were obfuscated using decoys with n key bits and locked using the point function with ibw key bits under the CAVM-MUL architecture using a total of $n + ibw$ key bits. These protected designs are also compared with those locked by both RLL and CASLock, where the

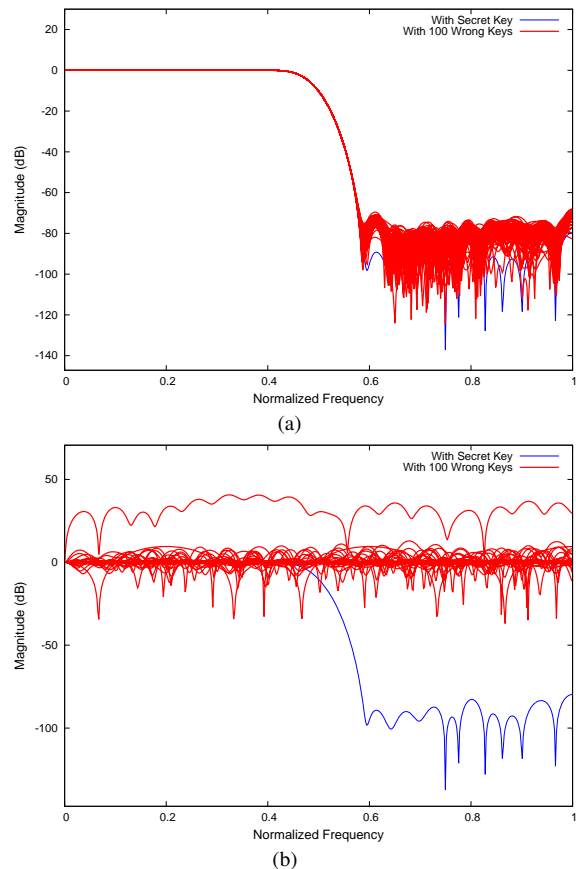


Fig. 14. Behavior of the FIR filter *Nielsen89*: (a) protected by the hybrid technique; (b) locked by RLL+CASLock.

number of RLL and CASLock key bits is $n - ibw$ and $2 * ibw$, respectively. This logic locking method was chosen because it generally generates a locked multiplier block with a small area as shown in Table VI. Table VIII presents the gate-level synthesis results of the CAVM designs protected by the hybrid technique and locked by both RLL and CASLock.

Observe from Table VIII that as the number of coefficients, n , increases, the hardware complexity of the protected and locked CAVM blocks generally increases. The hybrid protection technique generally leads to a design with a smaller area when compared to the RLL+CASLock method, where the gain reaches up to 32.6%. Note that on filters *Shi11_A* and *Maskell07*, the RLL+CASLock method leads to a locked design with a smaller area, since the bit-width of coefficients is small, enabling the synthesis tool to optimize the logic.

To find the impact of obfuscation techniques on the filter behavior, the Zero-Phase Frequency Response (ZPFR) of the FIR filter *Nielsen89* is obtained when the secret key and 100 randomly generated wrong keys are applied. Fig. 14 presents ZPFRs of FIR filters protected by the hybrid technique and locked by RLL+CASLock.

Observe from Fig. 14 that both obfuscation techniques may lead to a filter behavior different from the original one when a random wrong key is applied. While the filter behavior of the protected design under a wrong key is meaningful, but out of desired filter specification, the locked design exhibits an unmeaningful behavior under a wrong key due to the logic related to RLL key bits. Thus, the hybrid protection technique

may make the adversary believe that the filter behavior under the wrong key is actually the desired one.

VI. DISCUSSION

Other than the logic locking attacks used in this article, there exist Reverse Engineering (RE) and Side-Channel Analysis (SCA) techniques that can identify the filter coefficients in an obfuscated design. In [18], a machine learning tool that can determine the decoy selection method used in an obfuscated design was developed. The same work also proposed an RE technique that can identify filter coefficients hidden among decoys determined based on a decoy selection method. It was shown that if more than one decoy is used to obfuscate a filter coefficient, where the Hamming distance between each decoy and filter coefficient is 1, then the coefficient can be identified. In other cases, the RE technique was not capable of identifying original filter coefficients.

To the best of our knowledge, there exists no SCA technique proposed specifically to identify the original filter coefficients in an obfuscated filter design. The challenge for such a technique would be to understand how the synthesis tools embed the constants, i.e., filter coefficients and decoys, into the gate-level design using efficient methods, which optimize the hardware complexity of constant multiplications. This procedure would almost entail reverse engineering the algorithms used by the synthesis tools. In this case, it will be hard to reveal the filter coefficients from the power dissipation or delay values obtained from the obfuscated design since those data come from a logic combining both filter coefficients and decoys. Studying SCA and its efficiency to overcome obfuscation methods remains a formidable path for future research.

VII. CONCLUSIONS

This article focused on the obfuscation of digital FIR filters. Initially, it showed that the techniques previously proposed for the obfuscation of FIR filters are vulnerable to our SAT-based query attack, which applies several queries and proves that the found key bit value is the actual value of the related key bit in the secret key. Then, to secure an FIR filter design, it proposed the hybrid protection technique, which includes both obfuscation and locking with a point function. The proposed technique is applied to parallel direct and transposed forms of an FIR filter and its folded implementation. Experimental results clearly showed that the hybrid protection technique is competitive to prominent logic locking techniques in terms of hardware complexity and leads to obfuscated designs resilient to well-known attacks. It is also shown that the direct form FIR filter is a good candidate for secure filter implementation.

ACKNOWLEDGMENT

The authors would like to thank Nimisha Limaye and Satwik Patnaik for running our obfuscated designs on their tools and Mohammad Yasin, Leon Li, and Christian Pilato for fruitful discussions. The attacks were carried out in the High Performance Computing Centre of TalTech.

REFERENCES

- [1] Defence Science Board Task Force. (2015, February) On High Performance Microchip Supply Chain. [Online]. Available: <https://dsb.cto.mil/reports/2000s/ADA435563.pdf>
- [2] S. Amir, B. Shakya, D. Forte, M. Tehranipoor, and S. Bhunia, "Comparative Analysis of Hardware Obfuscation for IP Protection," in *GLSVLSI*, 2017, pp. 363–368.
- [3] A. B. Kahng, J. Lach, W. H. Mangione-Smith, S. Mantik, I. L. Markov, M. Potkonjak, P. Tucker, H. Wang, and G. Wolfe, "Watermarking Techniques for Intellectual Property Protection," in *DAC*, 1998, pp. 776–781.
- [4] Y. Alkabani, F. Koushanfar, and M. Potkonjak, "Remote Activation of ICs for Piracy Prevention and Digital Right Management," in *ICCAD*, 2007, pp. 674–677.
- [5] F. Koushanfar, "Provably Secure Active IC Metering Techniques for Piracy Avoidance and Digital Rights Management," *IEEE Transactions on Information Forensics and Security*, vol. 7, no. 1, pp. 51–63, 2012.
- [6] T. Hoque, R. S. Chakraborty, and S. Bhunia, "Hardware Obfuscation and Logic Locking: A Tutorial Introduction," *IEEE Design & Test*, vol. 37, no. 3, pp. 59–77, 2020.
- [7] L. Wanhhammar, *DSP Integrated Circuits*. Academic Press, 1999.
- [8] M. R. Muttaki, R. Mohammadivojdan, M. Tehranipoor, and F. Farahmandi, "HLock: Locking IPs at the High-Level Language," in *DAC*, 2021, pp. 79–84.
- [9] C. Pilato, A. B. Chowdhury, D. Sciuto, S. Garg, and R. Karri, "ASSURE: RTL Locking Against an Untrusted Foundry," *IEEE TVLSI*, vol. 29, no. 7, pp. 1306–1318, 2021.
- [10] S. A. Islam, L. K. Sah, and S. Katkooi, "High-Level Synthesis of Key-Obfuscated RTL IP with Design Lockout and Camouflaging," *ACM TODAES*, vol. 26, no. 1, 2020.
- [11] C. Pilato, F. Regazzoni, R. Karri, and S. Garg, "TAO: Techniques for Algorithm-Level Obfuscation during High-Level Synthesis," in *DAC*, 2018, pp. 1–6.
- [12] A. Sengupta, D. Roy, S. P. Mohanty, and P. Corcoran, "DSP Design Protection in CE through Algorithmic Transformation based Structural Obfuscation," *IEEE Transactions on Consumer Electronics*, vol. 63, no. 4, pp. 467–476, 2017.
- [13] R. S. Chakraborty and S. Bhunia, "RTL Hardware IP Protection Using Key-Based Control and Data Flow Obfuscation," in *International Conference on VLSI Design*, 2010, pp. 405–410.
- [14] Y. J. Yu and Y. C. Lim, "Optimization of Linear Phase FIR Filters in Dynamically Expanding Subexpression Space," *Circuits, Systems, and Signal Processing*, vol. 29, no. 1, pp. 65–80, 2010.
- [15] Y. Lao and K. K. Parhi, "Obfuscating DSP Circuits via High-Level Transformations," *IEEE TVLSI*, vol. 23, no. 5, pp. 819–830, 2015.
- [16] G. Bottegal, F. Farokhi, and I. Shames, "Preserving Privacy of Finite Impulse Response Systems," *IEEE Control Systems Letters*, vol. 1, no. 1, pp. 128–133, 2017.
- [17] L. Aksoy, Q.-L. Nguyen, F. Almeida, J. Raik, M.-L. Flottes, S. Dupuis, and S. Pagliarini, "High-Level Intellectual Property Obfuscation via Decoy Constants," in *IOLTS*, 2021, pp. 1–7.
- [18] L. Aksoy, A. Hepp, J. Baehr, and S. Pagliarini, "Hardware Obfuscation of Digital FIR Filters," in *DDECS*, 2022, pp. 68–73.
- [19] M. Ercegovic and T. Lang, *Digital Arithmetic*. Morgan Kaufmann, 2003.
- [20] L. Aksoy, P. Flores, and J. Monteiro, "ECHO: A Novel Method for the Multiplierless Design of Constant Array Vector Multiplication," in *ISCAS*, 2014, pp. 1456–1459.
- [21] L. Aksoy, E. O. Güneş, and P. Flores, "Search Algorithms for the Multiple Constant Multiplications Problem: Exact and Approximate," *Elsevier MICPRO*, vol. 34, no. 5, pp. 151–162, 2010.
- [22] L. Aksoy, P. Flores, and J. Monteiro, "Multiplierless Design of Folded DSP Blocks," *ACM TODAES*, vol. 20, no. 1, 2014.
- [23] M. Yasin, A. Sengupta, M. T. Nabeel, M. Ashraf, J. Rajendran, and O. Sinanoglu, "Provably-Secure Logic Locking: From Theory To Practice," in *ACM CCS*, 2017, pp. 1601–1618.
- [24] L. Aksoy, P. Flores, and J. Monteiro, "A Tutorial on Multiplierless Design of FIR Filters: Algorithms and Architectures," *Circuits, Systems, and Signal Processing*, vol. 33, no. 6, pp. 1689–1719, 2014.
- [25] M. Ercegovic and T. Lang, *Digital Arithmetic*. Morgan Kaufmann, 2003.
- [26] Y. Voronenko and M. Püschel, "Multiplierless Multiple Constant Multiplication," *ACM Transactions on Algorithms*, vol. 3, no. 2, 2007.
- [27] P. Tummelshammer, J. Hoe, and M. Püschel, "Time-Multiplexed Multiple-Constant Multiplication," *IEEE TCAD*, vol. 26, no. 9, pp. 1551–1563, 2007.

- [28] J. A. Roy, F. Koushanfar, and I. L. Markov, "EPIC: Ending Piracy of Integrated Circuits," in *DATE*, 2008, pp. 1069–1074.
- [29] J. Rajendran, M. Sam, O. Sinanoglu, and R. Karri, "Security Analysis of Integrated Circuit Camouflaging," in *ACM CCS*, 2013, pp. 709–720.
- [30] S. Dupuis and M.-L. Flottes, "Logic Locking: A Survey of Proposed Methods and Evaluation Metrics," *Journal of Electronic Testing*, vol. 35, pp. 273–291, 2019.
- [31] P. Subramanyan, S. Ray, and S. Malik, "Evaluating the Security of Logic Encryption Algorithms," in *HOST*, 2015, pp. 137–143.
- [32] M. Yasin, B. Mazumdar, J. Rajendran, and O. Sinanoglu, "SARLock: SAT Attack Resistant Logic Locking," in *HOST*, 2016, pp. 236–241.
- [33] Y. Xie and A. Srivastava, "Anti-SAT: Mitigating SAT Attack on Logic Locking," *IEEE TCAD*, vol. 38, no. 2, pp. 199–207, 2019.
- [34] B. Shakya, X. Xu, M. Tehranipoor, and D. Forte, "CAS-Lock: A Security-Corruptibility Trade-off Resilient Logic Locking Scheme," *IACR Transactions on CHES*, vol. 2020, no. 1, pp. 175–202, 2019.
- [35] A. Sengupta, M. Nabeel, N. Limaye, M. Ashraf, and O. Sinanoglu, "Truly Stripping Functionality for Logic Locking: A Fault-Based Perspective," *IEEE TCAD*, vol. 39, no. 12, pp. 4439–4452, 2020.
- [36] Q.-L. Nguyen, M.-L. Flottes, S. Dupuis, and B. Rouzeyre, "On Preventing SAT Attack with Decoy Key-Inputs," in *ISVLSI*, 2021, pp. 114–119.
- [37] H. Zhou, A. Rezaei, and Y. Shen, "Resolving the Trilemma in Logic Encryption," in *ICCAD*, 2019, pp. 1–8.
- [38] P. Chakraborty, J. Cruz, and S. Bhunia, "SAIL: Machine Learning Guided Structural Analysis Attack on Hardware Obfuscation," in *Asian HOST*, 2018, pp. 56–61.
- [39] L. Li and A. Orailoglu, "Piercing Logic Locking Keys through Redundancy Identification," in *DATE*, 2019, pp. 540–545.
- [40] A. Alaql, M. M. Rahman, and S. Bhunia, "SCOPE: Synthesis-Based Constant Propagation Attack on Logic Locking," *IEEE TVLSI*, vol. 29, no. 8, pp. 1529–1542, 2021.
- [41] L. Alrahis, S. Patnaik, F. Khalid, M. A. Hanif, H. Saleh, M. Shafique, and O. Sinanoglu, "GNNUnlock: Graph Neural Networks-based Oracleless Unlocking Scheme for Provably Secure Logic Locking," in *DATE*, 2021, pp. 780–785.
- [42] D. Sirone and P. Subramanyan, "Functional Analysis Attacks on Logic Locking," in *DATE*, 2019, pp. 936–939.
- [43] F. Yang, M. Tang, and O. Sinanoglu, "Stripped Functionality Logic Locking With Hamming Distance-Based Restore Unit (SFLD-hd) - Unlocked," *IEEE Transactions on Information Forensics and Security*, vol. 14, no. 10, pp. 2778–2786, 2019.
- [44] Z. Han, M. Yasin, and J. J. Rajendran, "Does Logic Locking Work with EDA Tools?" in *USENIX Security Symposium*, 2021, pp. 1055–1072.
- [45] J. Rajendran, Y. Pino, O. Sinanoglu, and R. Karri, "Security Analysis of Logic Obfuscation," in *DAC*, 2012, pp. 83–89.
- [46] Y. Shen and H. Zhou, "Double DIP: Re-Evaluating Security of Logic Encryption Algorithms," in *GLSVLSI*, 2017, pp. 179–184.
- [47] K. Z. Azar, H. M. Kamali, H. Homayoun, and A. Sasan, "SMT Attack: Next Generation Attack on Obfuscated Circuits with Capabilities and Performance Beyond the SAT Attacks," *IACR Transactions on CHES*, vol. 2019, no. 1, pp. 97–122, 2018.
- [48] C. Karfa, R. Chouksey, C. Pilato, S. Garg, and R. Karri, "Is Register Transfer Level Locking Secure?" in *DATE*, 2020, p. 550/555.
- [49] K. Shamsi, M. Li, T. Meade, Z. Zhao, D. Z. Pan, and Y. Jin, "AppSAT: Approximately Deobfuscating Integrated Circuits," in *HOST*, 2017, pp. 95–100.
- [50] K. Shamsi, M. Li, D. Z. Pan, and Y. Jin, "KC2: Key-Condition Crunching for Fast Sequential Circuit Deobfuscation," in *DATE*, 2019, pp. 534–539.
- [51] X. Xu, B. Shakya, M. M. Tehranipoor, and D. Forte, "Novel Bypass Attack and BDD-based Tradeoff Analysis Against All Known Logic Locking Attacks," in *Cryptographic Hardware and Embedded Systems*, vol. 10529, 2017, pp. 189–210.
- [52] N. Limaye, S. Patnaik, and O. Sinanoglu, "Fa-SAT: Fault-aided SAT-based Attack on Compound Logic Locking Techniques," in *DATE*, 2021, pp. 1166–1171.
- [53] —, "Valkyrie: Vulnerability Assessment Tool and Attack for Provably-Secure Logic Locking Techniques," *IEEE Transactions on Information Forensics and Security*, vol. 17, pp. 744–759, 2022.
- [54] B. Tan *et al.*, "Benchmarking at the Frontier of Hardware Security: Lessons from Logic Locking," 2020. [Online]. Available: <https://arxiv.org/abs/2006.06806>
- [55] FIRSuite. (2009) Suite of Constant Coefficient FIR Filters. [Online]. Available: <https://www.firsuite.net/>
- [56] P. Subramanyan. HOST'15 Code Material. [Online]. Available: <https://drive.google.com/file/d/19gYMK51VaynzPhCNJlvzmI0eJmF6kVU0/view>
- [57] H. K. Lee and D. S. Ha, "On the Generation of Test Patterns for Combinational Circuits," Department of Electrical Engineering, Virginia Polytechnic Institute and State University, Blacksburg, VA, Tech. Rep. 12-93, 1993.
- [58] A. Biere, K. Fazekas, M. Fleury, and M. Heisinger, "CaDiCaL, Kissat, Paracooba, Plingeling and Treengeling Entering the SAT Competition 2020," in *Proc. of SAT Competition 2020 – Solver and Benchmark Descriptions*, ser. Department of Computer Science Report Series B, vol. B-2020-1. University of Helsinki, 2020, pp. 51–53.
- [59] Y. Shen. DoubleDIP Code Material. [Online]. Available: https://github.com/YuanqiShen/Double_DIP
- [60] A. Alaql. SCOPE Code Material. [Online]. Available: <https://github.com/alaql89/SCOPE>
- [61] Kaveh Shamsi. Netlist Encryption and Obfuscation Suite. [Online]. Available: <https://bitbucket.org/kavehshm/neos/src/master/>

Levent Aksoy received his Ph.D. degree in electronics engineering from Istanbul Technical University (ITU), Istanbul, Türkiye, in 2009. He worked as a researcher at ITU and INESC-ID, Lisbon, Portugal. He also worked at Dialog Semiconductor, Istanbul, Türkiye, as a senior digital design engineer. Currently, he is a post-doctoral researcher at the Centre for Hardware Security at Tallinn University of Technology (TalTech), Tallinn, Estonia. His research interests include hardware security and CAD for VLSI circuits with emphasis on solving EDA problems using SAT models and optimization techniques.

Quang-Linh Nguyen currently works as a Design-for-Test engineer at STMicroelectronics, Grenoble, France. He received a M.S. degree in Integrated Circuits and Systems from University of Paris-Saclay, Paris, France, in 2018 and a PhD degree in Micro-Electronics from University of Montpellier, Montpellier, France, in 2022. His research interests include VLSI Design, Design-for-Trust, Design-for-Test and Hardware Security.

Felipe Almeida received his bachelor's degree in Computer Engineering from the Pernambuco University and a master's degree in Microelectronics from the Federal University of Rio Grande do Sul. He is currently affiliated with the Centre for Hardware Security at Tallinn University of Technology (TalTech) as a Ph.D. student. His research interests are on Hardware Security and Radiation Tolerant Circuits.

Jaana Raik is a professor of digital systems' verification at the Department of Computer Systems and the head of the Centre for Dependable Computing Systems of TalTech University, Estonia. Prof. Raik received his M.Sc. and Ph.D. degrees at TalTech in 1997 and in 2001, respectively. He has co-authored more than 200 peer-reviewed scientific publications. His research interests cover a wide area in electrical engineering and computer science domains including hardware test, functional verification, fault-tolerance and security as well as emerging computer architectures.

Marie-Lise Flottes is a researcher for the French National Research Center (CNRS). Since 1990, she has been conducting research at LIRMM, Montpellier, France. She received her Ph.D. degree in 1990 from the University of Montpellier. Her interests include design for testability, testability and dependability of secure circuits, test data compression and test management for SoC and SiP.

Sophie Dupuis has been an Associate Professor with LIRMM, Montpellier, France, since 2011. She received her M.Sc. and Ph.D. degrees in microelectronics and design on integrated circuits from the Pierre & Marie Curie University, Paris, France, in 2004 and 2009 respectively. Her current research interests are oriented towards hardware trust, the design of trusted circuits despite potential untrustworthy design steps in particular.

Samuel Pagliarini received the PhD degree from Telecom ParisTech, Paris, France, in 2013. He has held research positions with the University of Bristol, Bristol, UK, and with Carnegie Mellon University, Pittsburgh, PA, USA. He is currently a Professor at Tallinn University of Technology (TalTech) in Tallinn, Estonia where he leads the Centre for Hardware Security. His current research interests include many facets of digital circuit design, with a focus on circuit reliability, dependability, and hardware trustworthiness.